

## Fluid-Fluid Phononic Crystal with Elastic Coat Working in Audible Frequencies

Aleksandra KLIMEK

Wroclaw University of Science and Technology, Wyspiańskiego 27, 50-370 Wroclaw,  
aleksandra.klimek@pwr.edu.pl

### Abstract

Phononic Crystals are receiving rising attention in the field of modern acoustic materials. PCs are artificial structures of periodically arranged scatterers. Such a structure enables creating a band gap in which, due to the Bragg diffraction phenomenon, vibrations are restrained or even forbidden. In this paperwork, the fluid-fluid PC is tested and simulated - the scatterers are constructed of water cylinders with an ethylene propylene diene monomer coat (EPDM – a hyperelastic rubber) and are embedded in air. The band gap is calculated to emerge in the audible range of frequency. Every simulation is performed with the use of the finite element method.

**Keywords:** Phononic Crystal, band gap, Finite Element Method, viscoelasticity

### 1. Introduction

Phononic Crystals (PCs) are periodic structures of matrix-embedded scatterers in a host medium. The crystal mode of action is based on the difference between the inclusions and the medium acoustic impedance. Such composition reveals an intriguing behaviour. Its band structure may hold band gaps in which the acoustic wave propagation is prohibited.

Band gaps can be formed in the crystal band structure in two ways. First one is by the Bragg Diffraction and second is correlated with the localized modes inside the unit cell. Bragg diffraction occurs when scatterers repetitiously reflect acoustic wave repetitiously. The equidistant between every inclusion causes creation of a standing wave in the medium, thus confinement of the acoustic energy inside the PC.

The band structure depends on multiple parameters: the elastic properties of components, inclusions shape, lattice type (most common are: square, hexagonal and honeycomb) and spatial distribution of inclusions. The last one is described by lattice parameter  $a$  and filling factor  $\beta$ , which is the ratio of the volumes of the inclusion and the whole unit cell.

The periodicity of Phononic Crystals enables to derive the dispersion curves basing on single unit cell, i.e. with the application of Bloch Theorem. Primarily, for a given matrix, one must define the corresponding Brillouin Zone, which is a primitive, unit cell of a reciprocal lattice (which is, in turn, Fourier transform of regular lattice). In this work, the scatterers are arranged in a square lattice (Figure 1.a). The corresponding Brillouin Zone is presented in Figure 1.b. The dispersion curves may be obtained afterwards by calculating the eigenfrequencies for every wavevector.

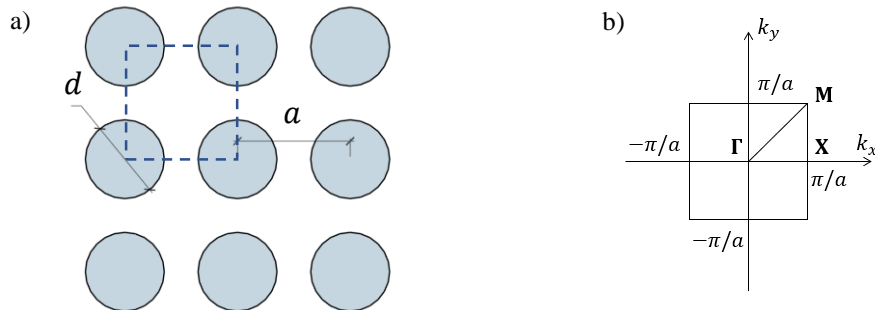


Figure 1. a) The square lattice. The dashed line represents unit cell; b) the corresponding first irreducible Brillouin Zone.  $\Gamma, X, M$  are highly symmetric points

In the following test, the host medium is air and the scatterers are constructed of water cylinders with an ethylene propylene diene monomer (EPDM rubber) coat. Due to the highly nonlinear nature of coat material and thus highly nonlinear behaviour of the water-coat inclusion pair, the prediction of dispersion curves is complicated. The Table 1. contains basic acoustic parameters of EPDM rubber.

Table 1. Basic properties of EPDM rubber [1]

Density [ $10^3 \frac{\text{kg}}{\text{m}^3}$ ]	Elastic Modulus [MPa]	Poisson Ratio	Sound Speed [ $\frac{\text{m}}{\text{s}}$ ]	Acoustic Impedance [ $10^3 \frac{\text{Pa s}}{\text{m}}$ ]
0.87	50.7	0.3	280	243.6

## 2. The FEM simulation results

The simulation was performed in COMSOL Multiphysics software. To simplify the calculations, it was assumed that the boundary between the medium (air) and cylinder (EPDM rubber) is hard. The Bloch-Floquet periodic boundary conditions were:

$$p_n = p_{n-1}e^{-ika} \tag{1}$$

where:

$p_{n-1}, p_n$  – the acoustic pressure on the left and right edge of unit cell respectively, in the  $x$  direction and on the bottom and top edge in the  $y$  direction;

$k$  – the wavevector component in the  $x$  or  $y$  direction respectively ( $k_x$  or  $k_y$ ).

Every geometric parameter of the simulation and real model are presented in the Table 2.

Table 2. Lattice geometric parameters

Quantity	Symbol	Unit	Value
Lattice parameter	$a$	[mm]	50
Water cylinder radius	$r_w$	[mm]	17.5
EPDM coat thickness	$d_E$	[mm]	4
Cylinder radius	$r_E$	[mm]	21.5
Filling factor	$\beta$	-	0.58
Rows number (among $y$ -axis)	-	-	6
Columns number (among $x$ -axis)	-	-	5

Resultant band structure for the first 5 eigenfrequencies is as shown on the Figure 2.

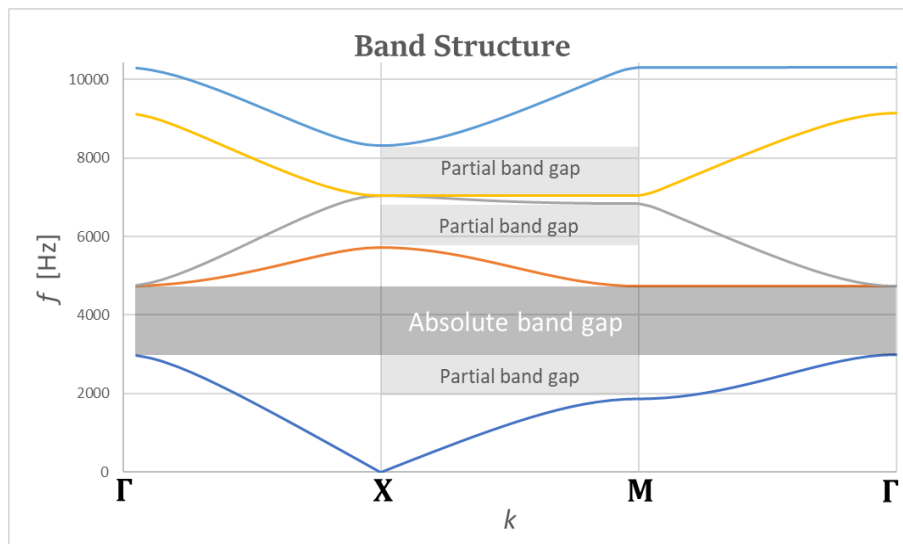


Figure 2. Band structure

In the given frequency range (0÷10 kHz) there is one absolute band gap (in every direction) and 3 partial band gaps, only for direction **X-M**. The Table 3 contains upper and lower frequency of every band gap.

Table 3. Band gaps frequencies

Band gap type	Partial (1)	Absolute	Partial (2)	Partial (3)
Lower frequency [Hz]	1872	2998	5726	7033
Upper frequency [Hz]	2998	4740	6831	8325

The sound pressure level distribution among the matrix acutely demonstrates the effects of absolute and partial bandgaps (Figure 3).

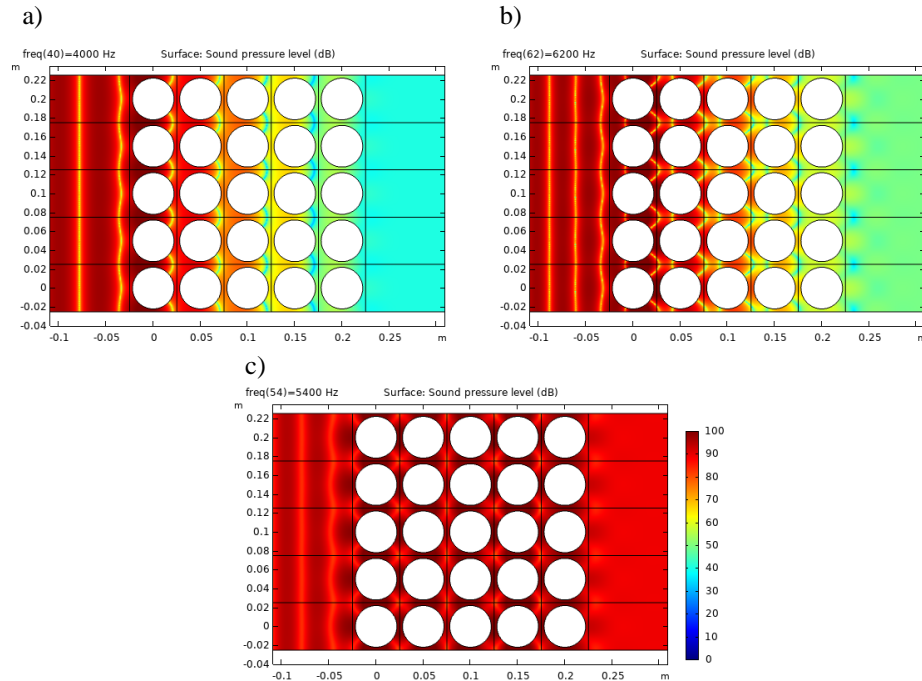


Figure 3. Sound pressure level distribution among the 5 columns of inclusions in the host medium domain (air).

- a) The frequency of 4000 Hz in the absolute band gap,
- b) The frequency of 6200 Hz in the partial band gap,
- c) The frequency of 5400 Hz (between the first two) in the conductive band.

The difference in SPL on the right edge of the crystal between conductive band and bandgap reaches 50 dB for the absolute and 40 dB for the partial band gap.

### 3. Test results

For the aim of this work, sonic crystal with every geometry parameter as given in Table 2. was constructed. Cylinders were fixed rigidly between two MDF boards to ensure its precise equidistant. There were *no* absorbing materials on the sides of the crystal. The research consisted of measuring the transmission loss between the no-PC and with the PC system (Figure 4.). In addition, a transmission loss with an empty coat (i.e. filled with air) was checked. The single broadband speaker was used to generate the sine sweep between 100 Hz and 10 kHz.

Due to rubber acoustic parameters, the measurements were expected to show shifting the band gap towards the lower frequencies. The frequency of local resonances of water cylinders *or* strings formed as a result of mounting the cylinder rigidly on both sides are located outside the frequency range in the study. However, according to the author's

opinion, the appearance of other resonances resulting from the superposition of rubber and water vibrations in the scatterer is believable. In such a case, in the resonance locations in the graph of transmission loss, one will be able to observe large differences between the curves representing water-filled and air-filled cylinders.

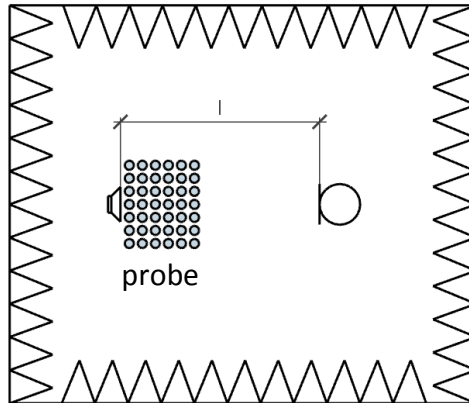


Figure 4. Measurement system diagram (top view).  $l$  is the distance between the broadband speaker and the microphone

The distance between microphone and speaker was variable. In total, measurements were taken for 16 positions of the microphone, with  $l$  between 50 cm and 2 m. Every transmission loss curve is 1/48 oct. smoothed and is a result of 3 measurements average. Selected representative results for  $l = 1$  m and  $l = 1.5$  m are in the Figure no 5 and 6 respectively.

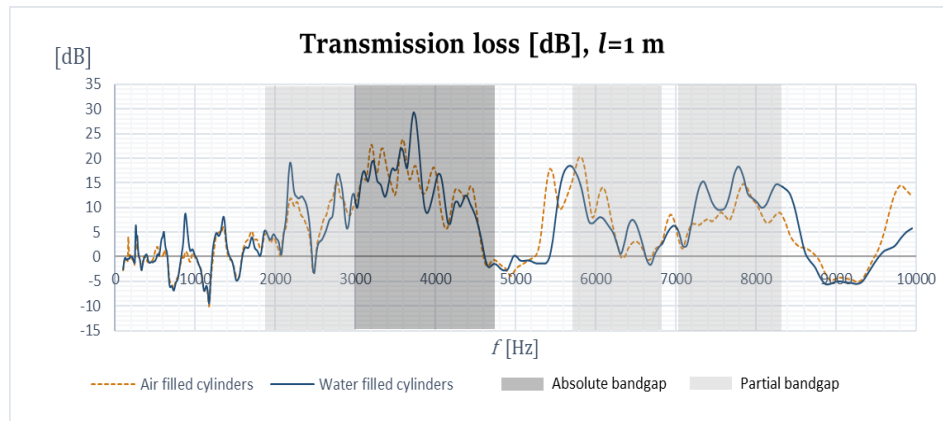


Figure 5. Transmission loss for  $l$  equal to 1 m

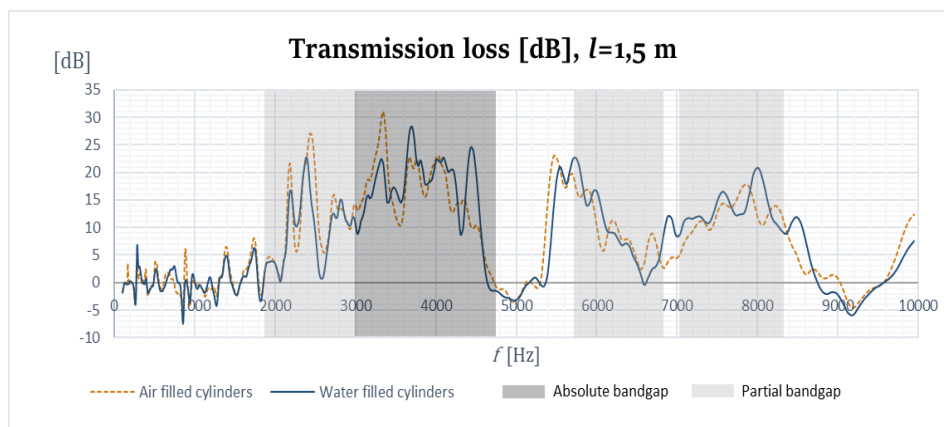


Figure 6. Transmission loss for  $l$  equal to 1.5 m

#### 4. Conclusions

The measurement results demonstrate a bandgap shift towards lower frequencies. This phenomenon is slightly more visible for the air-filled cylinders and becomes particularly evident for the absolute bandgap upper frequency (around 4.6 kHz), 2nd partial bandgap lower frequency (around 5.4 kHz) and narrow conductive band (around 6.6 kHz). The difference between air-filled cylinders and water-filled cylinders (around 5.4 kHz) allows supposing that this effect may occur due to the changed mass of the entire cylinder, and thus the creation of local resonance giving the impression of frequency shift. Other possible hypothesis explaining this effect is an impact of rubber impedance, which is not infinitely high. To confirm first or second hypothesis, in the future it would be necessary to compare the results with band structure of fluid-solid phononic crystal constructed of full EPDM cylinders.

The transmission loss curve is oscillating around 0 dB in the conductive band and reaches 20 dB in the presence of the bandgap (for single frequencies even 30 dB). Once more, this is an easily predictable effect, because the boundary between the scatterer and host medium was not completely hard. The lower difference in impedances must result in a weaker reflection of the wave between the scatterers.

Apart from the effect appearing around 5.4 kHz and described above, no evidence for localized modes was observed. Admittedly, there are single difference peaks (around 4 kHz for  $l = 1$  m graph and around 4.4 kHz for  $l = 1.5$  m), however, there is no constant difference for each microphone position. This allows to draw the conclusion that the observed differences do not result from the properties of the photonic crystal, but rather are the effect of the irregularity of the acoustic field in the measurement zone.

This work is an entry for further testing of viscoelastic materials in the application in photonic crystals and in acoustic metamaterials.

## References

1. Y. Fei, W. Fang, M. Zhong, H. Kadou et al., *Morphological Structure, Rheological Behavior, Mechanical Properties and Sound Insulation Performance of Thermoplastic Rubber Composites Reinforced by Different Inorganic Fillers*, *Polymers*, **10**(3) (2018) 276.
2. A. Khelif, A. Adibi, *Phononic Crystals, Fundamentals and Applications*, Springer, New York 2016.
3. P. A. Deymier, *Acoustic Metamaterials and Phononic Crystals*, Springer-Verlag Berlin Heidelberg, New York 2013.

